



# FACILE SOLVOTHERMAL SYNTHESIS OF VISIBLE LIGHT ACTIVE CDS NANOPARTICLES FOR THE PHOTODEGRADATION OF ROSE BENGAL (RB) DYE

Neha Jain<sup>1</sup>, Parmeshwar Lal Meena<sup>2</sup>, Deepika Choudhary<sup>3\*</sup>

## ABSTRACT

In this study, CdS nanophotocatalyst was prepared by low temperature solvothermal method for photodegradation of Rose Bengal (RB) dye in aqueous solutions in the presence of visible light photon. Further, synthesized CdS nanoparticles were characterized by various techniques such as Fourier Transform Infra-Red (FT-IR) Spectroscopy, X-Ray Diffraction (XRD), Scanning Electron Microscopy (SEM), and UV-Vis spectroscopy. The obtained CdSNPs shown hexagonal wurtzite structure with decent crystallinity, good optical features and exhibited admirable photocatalytic efficiency (98.50%) towards the photodegradation of Rose Bengal (RB) dye. Kinetic parameters for the degradation of RB with the prepared CdS nanoparticles were also reported and data well fitted to the pseudo-first-order kinetic model. The stability of CdS photocatalyst was remained constant and efficiency not decreased much more over the use of five cycles.

**Keywords:** -CdS, Nanophotocatalysts, Rose Bengal, Photodegradation, Kinetic parameters.

---

<sup>1,2,3\*</sup>Department of Chemistry, University of Rajasthan, Jaipur-302004 (India)

**\*Corresponding Author:** - Deepika Choudhary

\*Department of Chemistry, University of Rajasthan, Jaipur-302004 (India), Email-deepika028@gmail.com

**DOI:** 10.48047/ecb/2023.12.si10.00293

## 1. INTRODUCTION

In recent years, extensively increased industrialization due to fast growing rate of population and urbanization from which highly toxic and hazardous pollutants such as pesticides, herbicides, nitrophenols, and organic dyes are discharged into water resources. The elimination of these water contaminants is a difficult task [1]. Synthetic textile dyes with other industrial dye waste are considered one of the major water contaminants on the planet because of their offensive, poisonous, mutagenic and stable nature [2-4]. In the present scenario several techniques are utilizing to remove water contaminants, such as flocculation, coagulation, adsorption, and filtration, biological, but they are not much efficient, ecofriendly and economical [5,6] and the pollutants are not completely degraded in nonhazardous products, but transform into different forms, and at the same time produce a large amount of secondary toxic products as well [7].

The photo-degradation has been considered one of the efficient method for water treatment in compare to the traditional physicochemical and biological purification techniques which are insufficient for effective removal of pollutants [2, 8-12]. In recent years, photo-degradation of pollutants using semiconductors has been proven an effective process for the degradation of water pollutants especially organic dyes such as Rhodamine B [13,14] Brilliant cresyl blue, [15,16] Malachite green [17]. Several semiconductor nanomaterials including CdS nanoparticles have been used for effective heterogeneous photocatalytic degradation of organic dye pollutants in water [12, 18-20].

Last two decades, Nanoscience and nanotechnology have been gained much importance across the globe and thenanomaterials are using in various field for multiple applications such as biomedicine, devices, energy, solar cells, biotechnology, water treatment, delivering vaccines and drugs [21], treating communicable ailments, cancer detection, construction of scaffolds and in bioremediation.

Currently utilization of the II-VI group metal sulphide semiconductor nanoparticle is gained much attention as an important material for the photocatalysis for the proficient degradation of toxic pollutants including organic dyes, antibiotics, pesticides etc. under visible light illumination and to resolve the numerous aqueous environmental pollution problems [22-25]. Among

various metal sulfides II-VI semiconductor nanoparticles, a great attention has been showered on the cadmium sulphide (CdS) nanoparticles because of the admirable characteristics such as availability of discrete energy levels, tunable band gap, size dependent optical properties, well-developed synthetic protocols, easy preparation technique with good chemical stability and exciting photosensitivity [26]. CdS is a visible-light-driven photocatalyst that has an energy band gap of 2.4 eV [27]. It is extensively explored in various fields such as in detection of photochemical catalysis, visible radiations, light emitting diodes, solar cells, gas sensors, optoelectronic devices, luminescence devices, and environmental sensors [28-31]. Moreover, narrow band gap and negative edge potential of the conduction band of CdS has turned it into excellent semiconductor material for degradation of organic pollutants and H<sub>2</sub> generation using solar light [32,33]. Narrow band gap CdS allow to absorb solar-light photon effectively whereas higher surface area permits higher light photon absorption on the surfaces of CdS. So far, CdS nanoparticles numerous morphologies have been prepared using diverse methods such as chemical vapor deposition process [29], colloidal method [34], hydrothermal method [35], template method [36], sol gel template method [37], thermal decomposition method [38], solvothermal method [39], reversed micelle method [40], thermal evaporation method [41] and co-precipitation method [1].

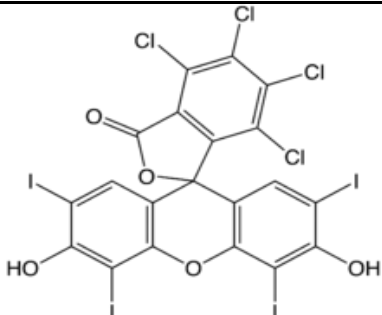
In the present work, CdS nanoparticles were synthesized by low temperature solvothermal method using 2-naphthylthiourea as source of (Sulphide) S<sup>2-</sup> ions in basic medium. The synthesized CdS nanoparticles were exploited as nanophotocatalyst for the photodegradation of Rose Bengal (RB) under visible light illumination which demonstrated exiting performance and stability.

## 2. MATERIALS AND METHOD

### 2.1. Materials used

Cadmium acetate, 2-naphthylthiourea, sodium hydroxide, hydrochloric acid, rose bengal (RB) and ethyl alcohol were used in preparation and experimental work in current study. For photocatalytic degradation, rose bengal was selected as a typical water contaminant in the present work. Rose bengal is frequently used in eye drops to stain injured conjunctival and corneal cells. The chemical formula and some properties of the RB dye are illustrated in Table 1.

**Table 1** The chemical structure and physicochemical properties of RB dye.

Structure	$\lambda_{\max}$ (nm)	MW (g/mol)	Molecular formula	Solubility (g/L)
	500-650	973.67	C <sub>20</sub> H <sub>4</sub> Cl <sub>4</sub> I <sub>4</sub> O <sub>5</sub>	100

## 2.2. Synthesis of CdS Nanoparticles

CdS nanoparticles were synthesized by simple and facile low temperature solvothermal method in alcoholic solution. In a typical process, 50 mL 0.1 M cadmium acetate and 50 mL of 0.1 M 2-naphthylthiourea (2-NTU) were prepared separately in ethyl alcohol and stirred for 30 min. After that 0.1 M 2-naphthylthiourea solution was mixed with cadmium acetate solution drop wise at constant stirring and pH of mixture was raised to 9

by addition of sodium hydroxide (1M) solution, yellow precipitate is appeared in mother liquor. The mother liquor along with precipitate was stirred for 2 h at 60°C and cool down to room temperature naturally. Then, the as-obtained suspension was centrifuged and washed several times with distilled water and finally with alcohol and dried at 70°C for 5 h in a hot air oven. The schematic synthesis protocol for the CdS nanoparticles is shown in Figure 1.

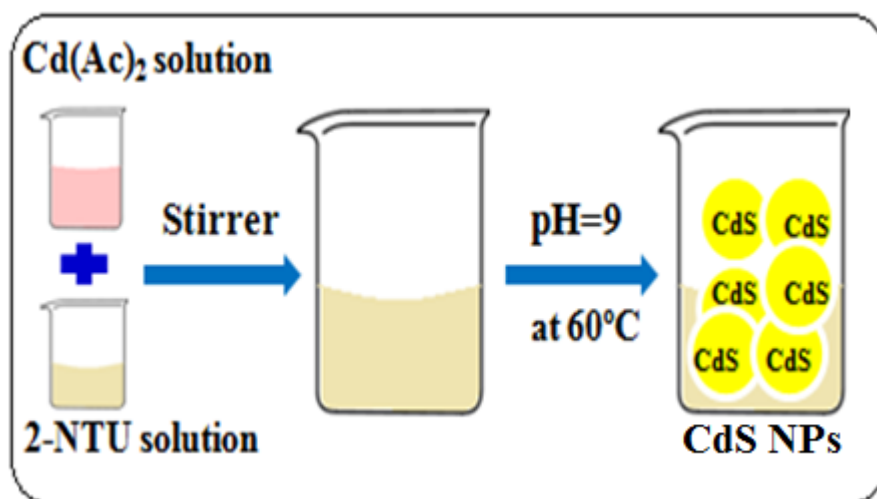


**Figure 1** Flow chart of synthesis of CdS nanoparticles.

## 2.3. Characterization

The morphological and structural analysis of the synthesized sample was carried out by Fourier Transform Infrared Spectroscopy (FTIR) Spectroscopy, Scanning Electron Microscopy (SEM) and X-ray diffraction (XRD). The optical properties were determined by using UV-Visible Spectroscopy.

## 2.4. Photocatalytic experiment

The photocatalytic activity of the synthesized CdS nanoparticles was studied by performing photodegradation experiments for Rose Bengal (RB) dye under visible light irradiation. The

optimization of reaction conditions was achieved by varying the catalyst dose amount, initial dye concentration, pH value of solution and reaction time. In a typical photocatalytic experiment, 50 mL of the dye solution of desired concentration containing the appropriate quantity of the catalyst at optimized pH was magnetically stirred in dark for 30 min to attain the adsorption-desorption equilibrium between dye and catalyst surface. 5 mL of the dye solution was withdrawn prior starting the irradiation. Aliquots (5 mL) were taken out from the dye solution at suitable time intervals during the light irradiation and centrifuged to remove catalyst, and the absorbance

intensity of RB dye solution was measured on a UV-spectrophotometer. To evaluate the auto-degradation of dye, standard experiment without using nano-catalyst was also performed using same reaction conditions. The percentage degradation of RB was estimated using equation (1) as given follows:

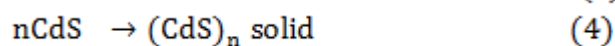
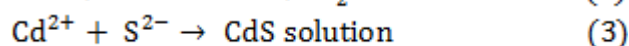
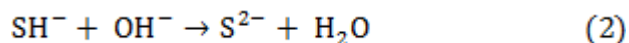
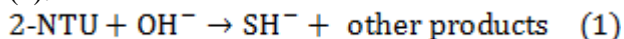
$$\text{Degradation efficiency (\%)} = \frac{C_0 - C_t}{C_0} \times 100 = \frac{A_0 - A_t}{A_0} \times 100 \quad (1)$$

Where  $C_0$  and  $C_t$  are the initial concentration and concentration at time (t), while  $A_0$  the absorbance of dye solutions at  $t=0$  while  $A_t$  is absorbance of dye solutions at  $t=t$ .

### 3. RESULTS AND DISCUSSION

#### 3.1. Synthesis of CdS Nanoparticles

The CdS nanoparticles were synthesized using low temperature solvothermal method in basic medium, in which  $\text{Cd}^{2+}$  and  $\text{S}^{2-}$  were supplied from cadmium acetate and 2-naphthylthiourea (2-NTU), respectively. In basic medium 2-naphthylthiourea produced  $\text{SH}^-$  ions which subsequently released  $\text{S}^{2-}$  that interacted with  $\text{Cd}^{2+}$  ions and form yellow colored CdS solution. The CdS particles agglomerated to generate CdS nanoparticles. The process of formation of CdS nanoparticles is represented in given reactions (1)-(4).



#### 3.2. Characterization

XRD pattern for synthesized CdS nanoparticle is shown in Figure 2. The diffraction peaks shown in XRD pattern at  $2\theta$  values of  $25.26^\circ$ ,  $26.5^\circ$ ,  $28.26^\circ$ ,  $38.85^\circ$ ,  $43.79^\circ$ ,  $48.02^\circ$ ,  $52.08^\circ$  and  $70.79^\circ$  can be indexed to the (100), (002), (101), (102), (110), (103), (112) and (211) crystal planes of hexagonal CdS, which clearly indicates that the as-prepared CdS contain high crystallinity, phase purity and have no any other impurity peaks.

The average crystalline size of the prepared nanoparticles is estimated from the Scherrer equation (2):

$$D = \frac{K\lambda}{\beta \cos\theta} \quad (2)$$

where  $D$  is the crystalline size,  $K$  is constant (0.9),  $\lambda$  is the wavelength of the incident X-ray (0.15417 nm),  $\theta$  is the diffraction angle and  $\beta$  is full width at half maximum (FWHM) of the highest intense (002) peak of the hexagonal phase of CdS. The evaluated average crystallite size is 18 nm for CdS nanoparticles.

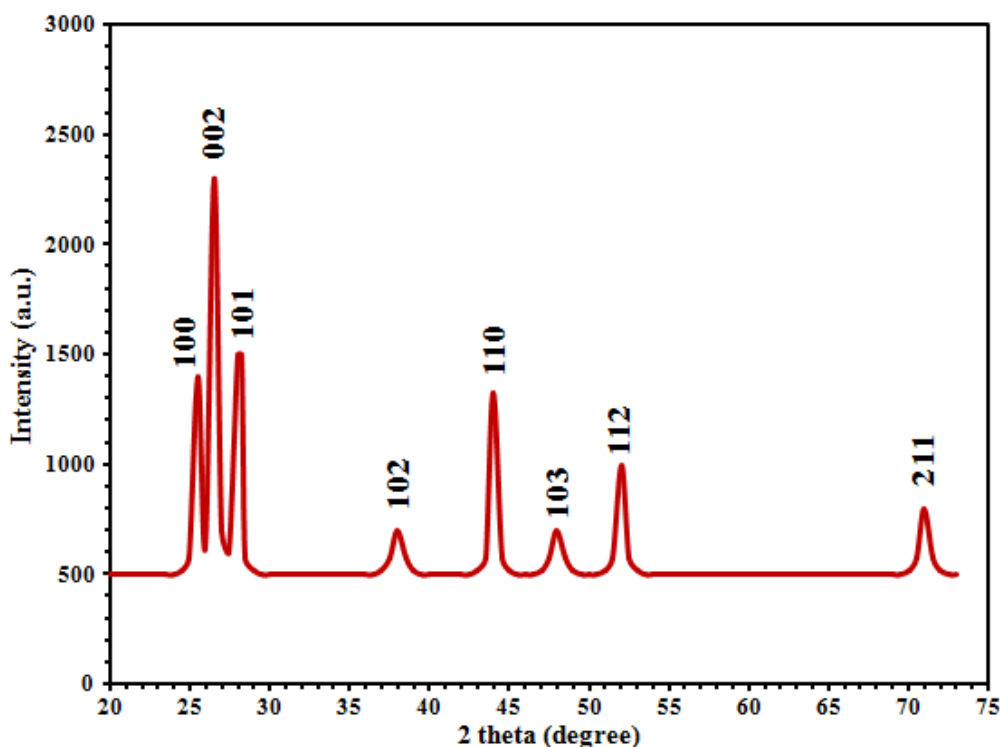


Figure 2 XRD pattern for CdS nanoparticles.

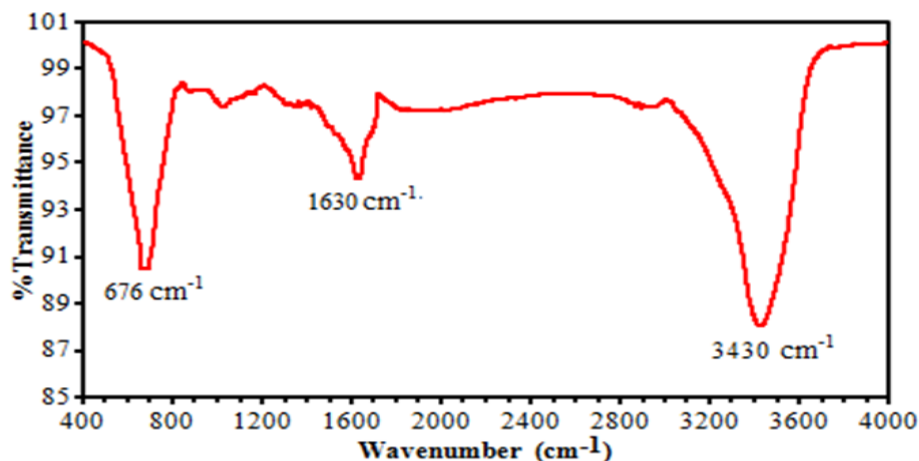


Figure 3 FTIR spectra for CdS nanoparticles.

FTIR is utilized to study the bonding and functionalities in the prepared product. The FTIR spectrum of synthesized CdS nanoparticles is shown in Figure 3. The absorption peaks noticed in spectrum at  $3430\text{ cm}^{-1}$  and  $1630\text{ cm}^{-1}$  are attributed to the  $\text{-OH}$  bonding vibrations of  $\text{H}_2\text{O}$  molecules adsorbed on the surface of CdS NPs.

An intense peak at  $400\text{-}700\text{ cm}^{-1}$  can be assigned to metal-sulphur (M-S) bond which confirms construction of CdS nanoparticles [42]. The peak observed at  $676\text{ cm}^{-1}$  in FTIR spectrum is

corresponding to the Cd-S bond [43, 44]. The SEM micrographs at various magnifications of synthesized sample are shown in Figure 4. The particles do not have definite shape, however seem like stone and possess rough surfaces. It might be due to more of a fine amorphous powder. The UV absorption spectrum of the synthesized CdS nanoparticles is revealed in Figure 5(a). The spectrum exhibited a distinct absorption peak at  $576\text{ nm}$ , which shows blue-shift as compared to the absorption peak of bulk CdS indicating quantum size effect.

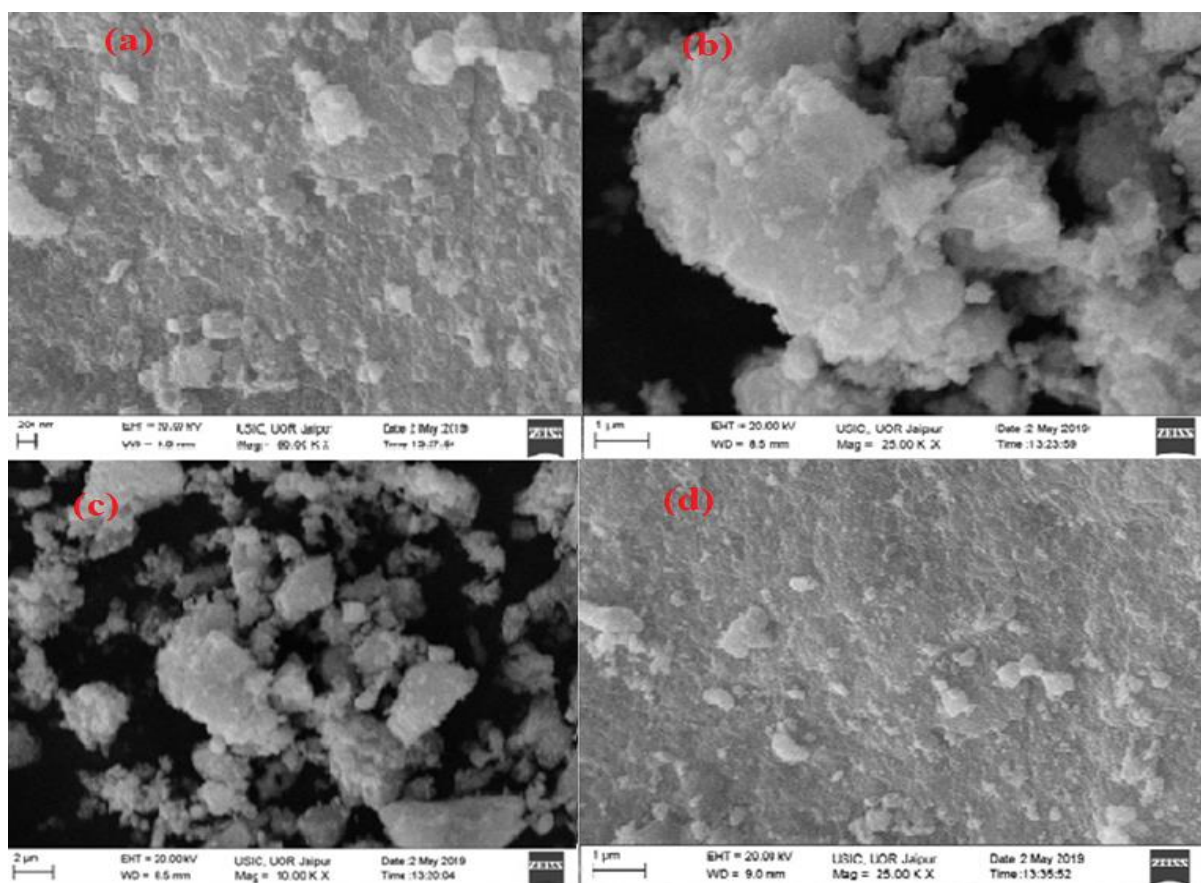


Figure 4 SEM images of the synthesized CdS nanoparticles.

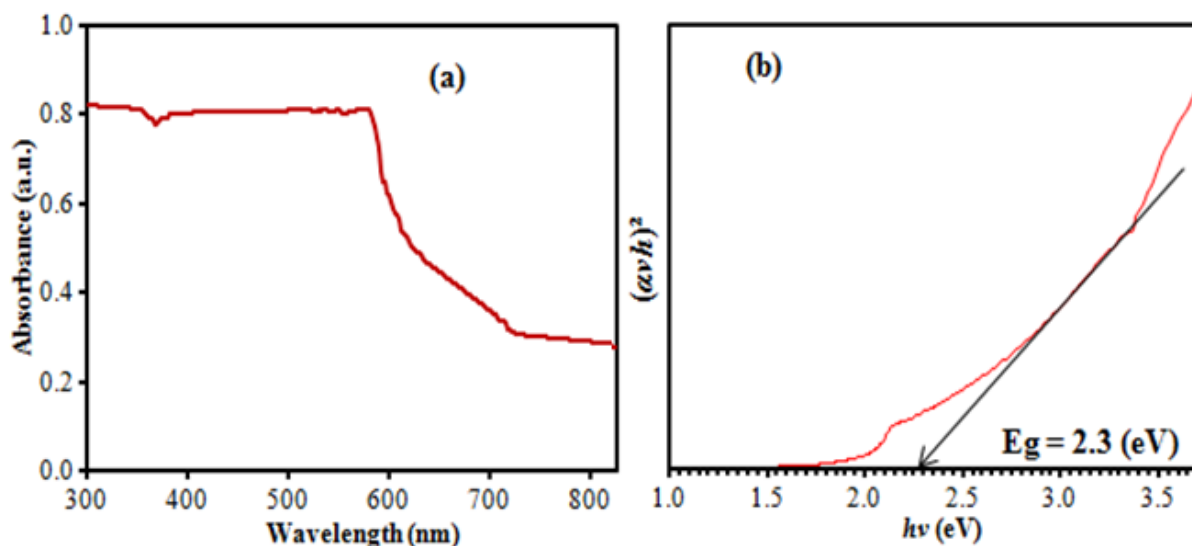


Figure 5(a)UV absorption spectra, and (b) bandgap value for synthesized CdS nanoparticles.

### 3.3. Bandgap calculation

The bandgap energy ( $E_g$ ) value can be evaluated from the UV–Vis absorption spectrum via a Tauc plot drawn between  $(\alpha h\nu)^2$  and  $(h\nu)$ . The optical bandgap energy for the prepared CdS nanoparticles was calculated using the Debye-Scherrer's relation as given by equation (3) [45].

$$(\alpha h\nu)^n = K(h\nu - E_g) \quad (3)$$

where  $K$  is a absorption coefficient,  $E_g$  is the bandgap of material,  $\nu$  is the frequency of the incident radiation and  $h$  is the Planck's constant, and the exponent  $n$  is 2 for direct band allowed transitions. The optical band gap energy was estimated by extrapolating the straight-line portion of  $(\alpha h\nu)^2$  vs.  $h\nu$  plot to  $h\nu$  axis at  $\alpha=0$  as shown in Figure 5(b). The obtained band gap for CdS nanoparticles is 2.3.eV.

### 3.4. Photocatalytic Degradation of RB Dye

The photodegradation performance of the synthesized CdS nanoparticles was investigated by performing photo-degradation experiments of Rose Bengal (RB) dye using visible light. The standard experiments were also performed by illuminating dye aqueous solution without using CdS NPs and using CdS NPs in the dark.

Investigation of the samples in both cases do not show any significant degradation of the dye. As shown in Figure 6(a) the absorption peak of RB dye at 553 nm is repeatedly falling with time due to photo-degradation of RB dye into non-hazardous products and the pink color of the dye solution completely changed to colorless after the 80 min of light irradiation and no absorption peak noticed, which indicated the complete photodegradation of RB dye by CdS nanoparticles.

The degradation efficiency of synthesized CdS catalyst for RB dye under visible light irradiation was determined to be 98.50% after 80 min of light irradiation. It is suggesting that CdS demonstrated good photocatalytic activity in this process. Figure 6(b) portrays the change in RB concentration ( $C_t/C_0$ ) with time over CdS nanoparticles under illumination with visible light and for blank RB solution in the dark. It can be observed from Figure 6(b) that the RB solution in dark with a catalyst not degraded appreciably, it only adsorbed on the surface of catalyst. However, in absence of catalyst it is self-degraded slowly under visible light illumination. The enhanced photocatalytic performance of CdS nanoparticles may be due to the small size and large specific surface area.

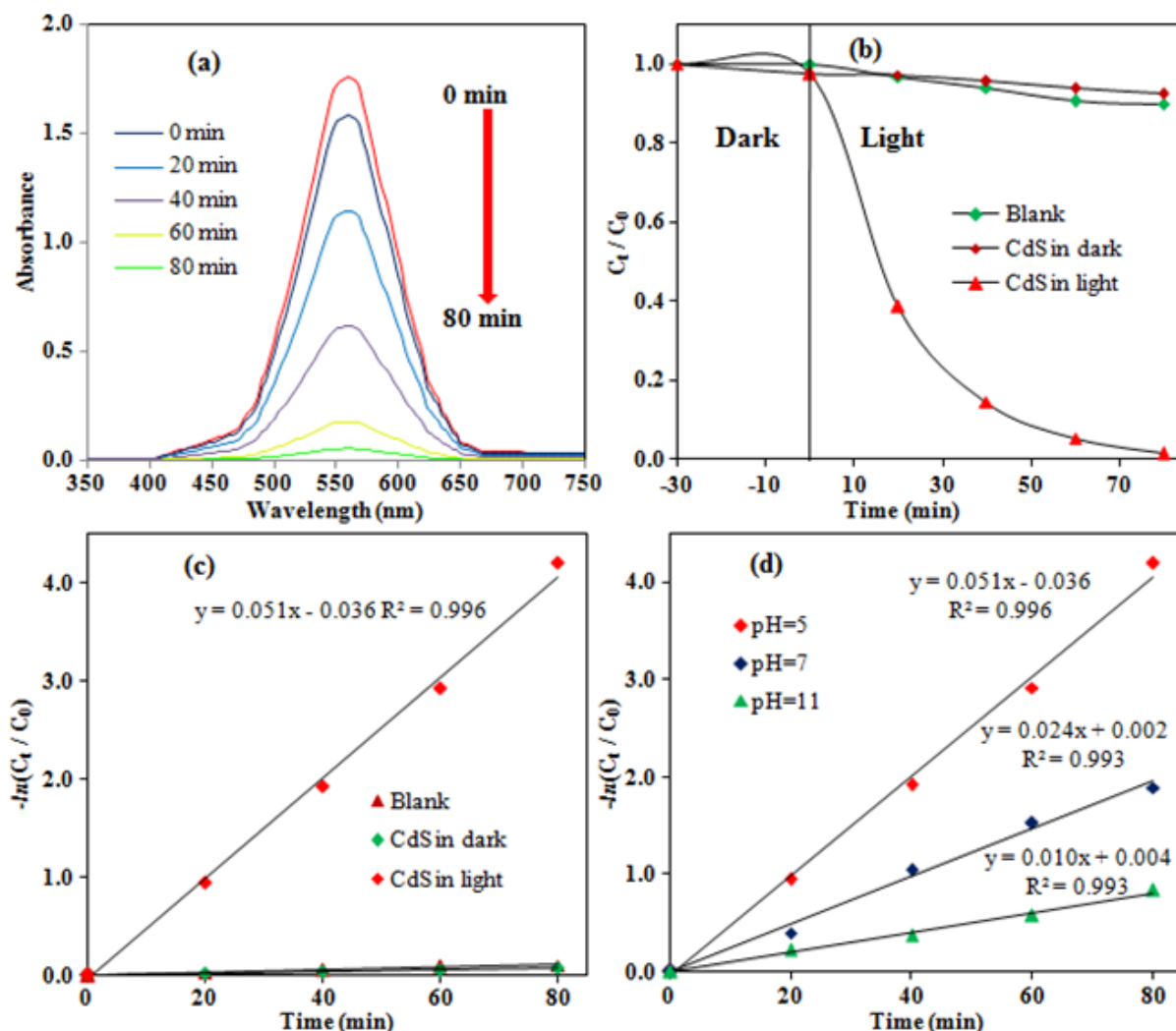


**Figure 6** (a) Time-dependent UV-Vis spectrum of Rose Bengal (RB) dye solution, (b) The degradation of (RB) dye in the presence of CdS nanoparticles under visible light, (c) Pseudo first order kinetic plots for the photocatalytic degradation of RB dye at optimized reaction parameters, and (d) Pseudo first order kinetic plots showing the effect of pH of solution on the kinetics of RB photodegradation.

### 3.5. Kinetics of Photodegradation of RB Dye

The reaction kinetics of photodegradation of RB by with the synthesized CdS nanophotocatalyst under visible light illumination at optimized reaction parameters was investigated as displayed in Figure 6(c). The degradation reactions of CdS nanoparticles with RB dye followed pseudo-first-order kinetics. The measured experimental data well fitted with the pseudo-first-order kinetic model as given below Eq (4):

$$\ln\left(\frac{A_0}{A_t}\right) = \ln\left(\frac{C_0}{C_t}\right) = kt \quad (4)$$

where,  $k$  ( $\text{min}^{-1}$ ) is the pseudo-first-order kinetic rate constant,  $A_0$  and  $A_t$  are the initial absorbance

and absorbance at time  $t$  of the RB dye, and  $C_0$  and  $C_t$  are dye concentrations at  $t=0$  and  $t=t$  time, respectively. The rate constants  $k$  for the pseudo first-order reaction is determined from the slope of the graph drawn  $-\ln(C_t/C_0)$  as a function of the irradiation time ( $t$ ). The plot for pseudo first-order photodegradation reaction of RB dye is shown in Figure 6(c) with corresponding slopes of the fitting lines. The rate constant obtained for photodegradation reaction of RB in the presence of catalyst ( $0.0512 \text{ min}^{-1}$ ) is very much greater than the self-degradation reaction in absence of catalyst ( $0.00142 \text{ min}^{-1}$ ) under the light illumination. The determined values for the rate constant ( $k$ ) and correlation coefficient ( $R^2$ ) are tabulated in Table 2.

**Table 2** Reaction kinetics parameters for RB photodegradation by CdS photocatalyst

Reaction condition	Rate constant (min <sup>-1</sup> )	Correlation coefficient (R <sup>2</sup> )
In light without catalyst	0.00142	0.977
In dark with catalyst	0.00084	0.916
In light with catalyst	0.0512	0.996

**Table 3** Effect of pH on reaction kinetics parameters for RB photodegradation by CdS photocatalyst

pH value	Rate constant (min <sup>-1</sup> )	Correlation coefficient (R <sup>2</sup> )
5	0.0512	0.996
7	0.0244	0.993
11	0.01007	0.993

In order to investigate the effect of solution pH on kinetics of RB photodegradation by the CdS photocatalyst, the photocatalysis reactions were carried out in the pH range of 5 to 11 keeping constant the dose amount of catalyst and dye concentration at room temperature. The influence of pH on kinetics of photodegradation reaction is illustrated in Figure 6(d) and the results are tabulated in Table 3. It can be observed from the results that rate constant values are decreasing with the increase of solution pH, the highest value of rate constant (0.0512 min<sup>-1</sup>) was obtained for pH=5 while the lowest for pH=11(0.01007 min<sup>-1</sup>). The higher value of rate constant at 5 pH was reported due to the enhanced adsorption of anionic RB dye on the surface of CdS photocatalyst due to positive charge on surface at this pH range [46]. On the contrary, in the basic medium (pH 11), surface of CdS photocatalyst carries negative charge that repels the anionic dye due to this rate constant value determined lower.

### 3.6. Photodegradation Mechanism

The activation of CdS nanocatalyst by light photon ( $h\nu$ ) absorption produces electron and holes at the valance band (VB) of catalyst, which are powerful oxidizing and reducing agents, respectively. The photogenerated holes stay at the VB while the electrons jump at the conduction band (CB) from where they transfer to the surface of catalyst, and trap by dissolved oxygen molecules produce hydroxyl free radicals ( $\cdot\text{OH}$ ), while the holes stay at VB also transfer to the surface of catalyst and inter with the water molecules to generate superoxide radical anions ( $\cdot\text{O}_2^-$ ). These produced highly active free radical species interact with dye molecules and degrade into intermediate products, which finally decompose into non-hazardous inorganic  $\text{CO}_2$  and  $\text{H}_2\text{O}$  molecules. The proposed possible photodegradation mechanism for the RB dye in presence of CdS catalyst is schematically represented in Figure 7 and explained by given in Eqs (5)-(10).

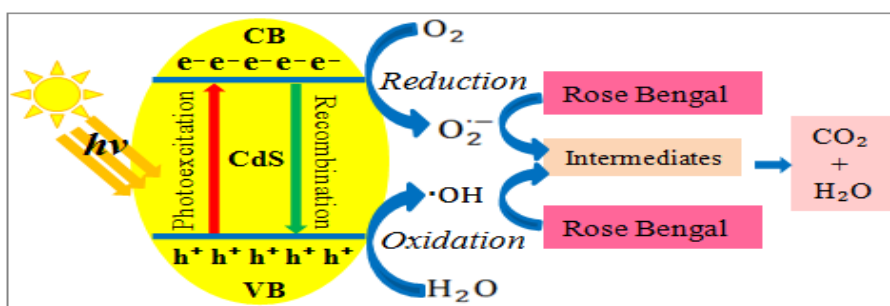
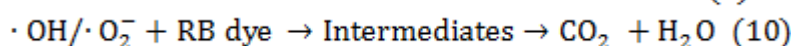
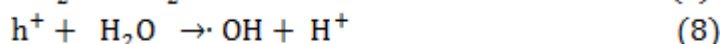
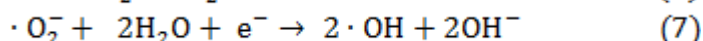
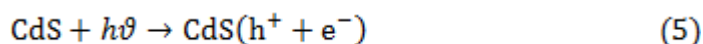


**Figure 7** Schematic representation of the possible mechanism involved in photocatalysis.





### 3.7. Reusability of Catalyst

The stability is a very important characteristic besides photocatalytic activity of any photocatalyst for the practical applications. The stability of the synthesized CdS photocatalyst was also investigated. The photocatalytic degradation experiment for RB dye was repeated applying similar procedures as mentioned in experimental section except catalyst for five cyclic runs. After each cycle of the photodegradation study the photocatalyst was recovered by centrifugation, washed with ethanol and water several times and dried in an oven, then reused for the next cycle. The photodegradation efficiency of CdS nanoparticles in five cyclic runs was determined to

be 98.50%, 95.54%, 92.07%, 88.50% and 85.05% for first, second, third, fourth and fifth cycles, respectively as shown in Figure 8. It can be seen from the results that the photocatalytic activity of the CdS nanoparticles is not significantly decreased and activity remained almost constant over five cycles of RB degradation.

The reduction in the competence of the CdS NPs might be due to the adsorption of dye molecules on the active locations of NPs [47]. Moreover, the assembling of the NPs when they are separated from solution possibly one more reason for the decline of the performance of the photocatalysts [48].

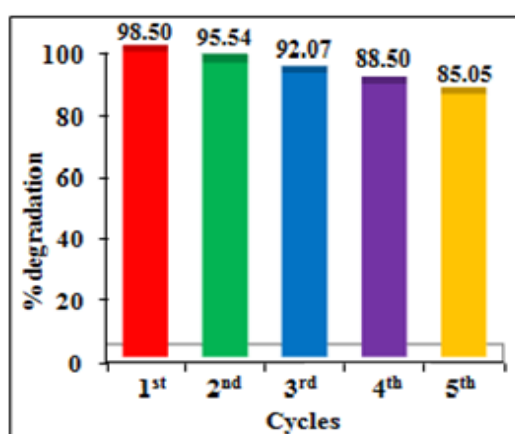


**Figure 8** Bar chart showing reusability of the CdS photocatalyst for the photodegradation of RB for five cycles under white light irradiation.

The catalytic performance of the obtained CdS NPs was compared with various formerly developed catalysts which have been used for decolorization of different dyes and demonstrated in Table 4. From the comparative analysis it can

be clearly indicated that CdS NPs prepared in the current study has shown good photo-degradation performance for the degradation of RB dye with visible light photons.

**Table 4.** Comparison study of catalytic performance of CdS NPs with other formerly developed catalysts

Catalysts	Light source	Time (min)	% Degradation	Organic Dye	References
ZnO/Ag <sub>2</sub> O NPs	UV	40	96%	Methylene blue (MB)	[49]
Gd-doped MnFe <sub>2</sub> O <sub>4</sub>	Visible	70	96.35%	Methylene blue (MB)	[50]
p-Bi <sub>2</sub> O <sub>3</sub> /n-ZnO	Visible	60	93%	alizarin red (AR)	[51]
CdS	Visible	80	99%	Congo red (CR)	[52]
CdS	Visible	240	100%	Reactive red 141 (RR141)	[52]
CdS	Visible	240	95%	Reactive red 141 (RR141)	[53]
TiO <sub>2</sub>	UV	90	90%	Reactive red 141 (RR141)	[54]
CdS	Visible	80	98.50%	Rose bengal (RB)	<b>This work</b>

## 4. CONCLUSIONS

Cadmium sulphide nanoparticles were synthesized via a simple and facile low temperature solvothermal method, using 2-naphthylthiourea as sulphide ion sources. The structural,

morphological and optical characteristics of the synthesized CdS nanoparticles were characterized by Fourier Transform Infra-Red (FT-IR) Spectroscopy, X-Ray Diffraction (XRD), Scanning Electron Microscopy (SEM), and UV-

vis spectroscopy. The prepared CdS photocatalyst demonstrated hexagonal structure with high crystallinity, excellent optical properties and exhibited admirable photocatalytic efficiency toward photodegradation of RB. Kinetic parameters for the degradation of RB in presence of CdS nanoparticle were reported. The experimental data well fitted with the pseudo-first-order kinetic model which confirmed that the photodegradation of RB dye followed pseudo first order kinetics. The stability of CdS photocatalyst was remained constant and efficiency not decreased much more over the use of five cyclic run of reuse. The dye degradation under optimum conditions on 80 min of visible light irradiation was determined to be 98.50% and the photodegradation efficiency of CdS nanoparticles after fourth run of reuse was determined 85.05% which demonstrated good stability and reusability of prepared CdS nanoparticles.

#### Acknowledgements

Authors are grateful to the Department of Chemistry and USIC, University of Rajasthan, Jaipur (India) for technical assistance and providing necessary research facilities.

#### Conflicts of Interest

Author proclaims no conflicts of interest.

#### 5. REFERENCES

1. Ayodhya D. & Veerabhadarm G. 2019 Facile fabrication, characterization and efficient photocatalytic activity of surfactant free ZnS, CdS and CuS nanoparticles. *Journal of Science: Advanced Materials and Devices* 4, 381-391.
2. Ma L.-L., Sun H.-Z., Zhang Y.-G., Lin Y.-L., Li J.-L., Wang E.-K., Yu Y., Tan M. & Wang J.-B. 2008 Preparation, characterization and photocatalytic properties of CdS nanoparticles dotted on the surface of carbon nanotubes. *Nanotechnology* 19, 115709-8.
3. Mahmoodi N. M., Arami M., Limaee N. Y. & Tabrizi N. S. 2005 Decolorization and aromatic ring degradation kinetics of Direct Red 80 by UV oxidation in the presence of hydrogen peroxide utilizing TiO<sub>2</sub> as a photocatalyst. *Chemical Engineering Journal* 112, 191-196.
4. Papi S., Koprivanac N., Bozi A. L. & Metes A. 2004 Removal of some reactive dyes from synthetic wastewater by combined Al (III) coagulation/carbon adsorption process. *Dyes and Pigments* 62, 291-298.
5. Kumar A., Kumar A., Sharma G., Alaa H., Naushad M., Ghfar A.A., Guo C. & Stadler F. J. 2018 Biochar-templated g-C<sub>3</sub>N<sub>4</sub>/Bi<sub>2</sub>O<sub>3</sub>/CoFe<sub>2</sub>O<sub>4</sub> nano-assembly for visible and solar assisted photo-degradation of paraquat, nitrophenol reduction and CO<sub>2</sub> conversion. *Chem. Eng. J.* 339, 393-410.
6. Sharma G., Gupta V.K., Agarwal S., Bhogal S., Naushad M., Kumar A. & Stadler F.J., 2018a Fabrication and characterization of trimetallic nano-photocatalyst for remediation of ampicillin antibiotic. *J. Mol. Liq.* 260, 342-350.
7. Ayodhya D., Venkatesham M., Kumari A.S., Reddy G.B., Ramakrishna D. & Veerabhadarm G. 2016 Photocatalytic degradation of dye pollutants under solar, visible and UV lights using green synthesised CuS nanoparticles. *J. Exp. Nanosci.* 11, 418-432.
8. Ozacar M. & Engil I. A. 2003 Adsorption of reactive dyes on calcined alunite from aqueous solutions. *Journal of Hazardous Materials* 98, 211-224.
9. Sun J., Wang X., Sun J., Sun R., Sun S. & Qiao L. 2006 photocatalytic degradation and kinetics of orange G using nano-sized Sn (IV)/TiO<sub>2</sub>/AC photocatalyst. *Journal of Molecular Catalysis A: Chemical* 260, 241-246.
10. Ki R., Stucki S., & Carcer B. 1991 Electrochemical waste water treatment using high overvoltage anodes. Part I: physical and electrochemical properties of SnO<sub>2</sub> anodes. *Journal of Applied Electrochemistry* 21, 14-20.
11. Cheng Y., Sun H., Jin W. & Xu N. 2007 photocatalytic degradation of 4-chlorophenol with combustion synthesized TiO<sub>2</sub> under visible light irradiation. *Chemical Engineering Journal* 128, 127-133.
12. Zhiyong Y., Keppner H., Laub D., Mielczarski E., Mielczarski J., Kiwi-Minsker L., Renken A. & Kiwi, J. 2008 Photocatalytic discoloration of methyl orange on innovative parylene-TiO<sub>2</sub> flexible thin films under simulated sunlight. *Applied Catalysis B: Environmental*, 79, 63-71.
13. Parmeshwar Lal Meena, Krishna Poswal, Ajay Kumar Surela and Jitendra Kumar Saini (2021a), Facile synthesis of ZnO/CuO/Ag<sub>2</sub>O ternary metal oxide nanocomposite for effective photodegradation of organic water pollutants. *Water Science & Technology.* 84(9), 2615 doi: 10.2166/wst.2021.431
14. Parmeshwar Lal Meena, Krishna Poswal, Ajay Kumar Surela, Bhanupriya Mordhiya and Kamod Singh Meena (2023a), Ag<sub>2</sub>O Adorned ZnO Nanostructures: Cooperative and

- Sustainable Nanomaterial System for Effective Reduction and Mineralization of Hazardous Water Pollutants, *Environmental Science and Pollution Research*, 30, 68770–68791. <https://doi.org/10.1007/s11356-023-27215-7>
15. Parmeshwar Lal Meena, Krishna Poswal and Ajay Kumar Surela (2021b), Fabrication of ZnO/CuO Hybrid Nanocomposite for Photocatalytic Degradation of Brilliant Cresyl Blue (BCB) Dye in Aqueous Solutions, *J. Water Environ. Nanotechnol.* 6(3):196-211. <https://doi.org/10.22090/jwent.2021.03.001>
  16. Parmeshwar Lal Meena, Krishna Poswal, Ajay Kumar Surela and Jitendra Kumar Saini (2023b), Synthesis of graphitic carbon nitride/zinc oxide (g-C<sub>3</sub>N<sub>4</sub>/ZnO) hybrid nanostructures and investigation of the effect of ZnO on the photodegradation activity of g-C<sub>3</sub>N<sub>4</sub> against the brilliant cresyl blue (BCB) dye under visible light irradiation, *Advanced Composites and Hybrid Materials*, 6:16. <https://doi.org/10.1007/s42114-022-00577-1>
  17. Parmeshwar Lal Meena, Krishna Poswal, Ajay Kumar Surela (2022a), Facile Synthesis of ZnO Nanoparticles for the Effective Photodegradation of Malachite Green (MG) Dye in Aqueous Solution. *Water and Environment Journal*, DOI: 10.1111/wej.12783.
  18. Frayne S. H., Barnaby S. N., Nakatsuka N. & Banerjee I. A. 2012 Growth and properties of CDSE nanoparticles on ellagic acid biotemplates for photodegradation applications. *Materials Express* 2, 335-343.
  19. Parmeshwar Lal Meena, Ajay Kumar Surela, Krishna Poswal, Jitendra Kumar Saini, Lata Kumari Chhachhia (2022c). *Millettia Pinnata* Plant Pod Extract-Mediated Synthesis of Bi<sub>2</sub>O<sub>3</sub> for Degradation of Water Pollutants. *Environmental Science and Pollution Research*, 29:79253–79271 <https://doi.org/10.1007/s11356-022-21435-z>
  20. Parmeshwar Lal Meena, Ajay Kumar Surela, Krishna Poswal, Jitendra Kumar Saini, Lata Kumari Chhachhia (2022b), Biogenic Synthesis of Bi<sub>2</sub>O<sub>3</sub> Nanoparticles Using Cassia fistula Plant Pod Extract for the Effective Degradation of Organic Dyes in Aqueous Medium. (2022), *Biomass Conversion and Biorefinery*, DOI:10.1007/s13399-022-02605-y
  21. Du J., Fu L., Liu Z., Han B., Li Z., Liu Y., Sun Z. & Zhu D. 2005 Facile route to synthesize multi-walled carbon nanotube/zinc sulfide heterostructures: Optical and electrical properties. *Journal of Physics and Chemical Biology* 109, 12772–12776.
  22. Sharma G., Kumar A., Naushad M., Kumar A., Al-Muhtaseb A.H., Dhiman P., Ghfar A.A., Stadler F.J. & Khan M.R. 2018b Photoremediation of toxic dye from aqueous environment using monometallic and bimetallic quantum dots based nanocomposites. *J. Clean. Prod.* 172, 2919-2930.
  23. Ayodhya D. & Veerabhadram G. 2018a Hydrothermally generated and highly efficient sunlight responsive SiO<sub>2</sub> and TiO<sub>2</sub> capped Ag<sub>2</sub>S nanocomposites for photocatalytic degradation of organic dyes. *J. Environ. Chem. Eng.* 6, 311-324.
  24. Ayodhya D. & Veerabhadram G., 2018b Ternary semiconductor Zn<sub>x</sub>Ag<sub>1-x</sub>S nanocomposites for efficient photocatalytic degradation of organophosphorus pesticides. *Photochem. Photobiol. Sci.* 17, 1429-1442.
  25. Shahi, S.K. Kaur N., Sandhu S., Shahi J.S. & Singh V. 2017 Influences of a new templating agent on the synthesis of coral-like TiO<sub>2</sub> nanoparticles and their photocatalytic activity. *J. Sci. Adv. Mater. Devices* 2, 347-353.
  26. Antolini F., Pentimalli M., Di Luccio T., Terzi R., Schioppa M., Re M. & Tapfer L. 2005 Structural characterization of CdS nanoparticles grown in polystyrene matrix by thermolytic synthesis. *Materials Letters* 59(24), 3181-3187.
  27. Wang D.J., Li D.S., Li G., Fu F., Zhang Z.P. & Wei Q.T. 2009 *J. Phys. Chem. C* 113, 5984.
  28. Chen C. C., Herhold A. B., Johnson C. S. & Alivisatos A. P. 1997 Size dependence of structural metastability in semiconductor nanocrystals. *Science* 276 (5311), 398-401.
  29. Barrelet C.J., Wu Y., Bell D.C. & Lieber C.M. 2003 Synthesis of CdS and ZnS nanowires using single-source molecular precursors. *J. Am. Chem. Soc.* 125, 11498–11499.
  30. Zhao P.T. & Huang K.X. 2008 Preparation and characterization of netted sphere-like CdS nanostructures. *Cryst. Growth Des.* 8, 717–722.
  31. Dongre J. K., Nogriva V. & Ramrakhiani M. 2009 Structural, optical and photoelectrochemical characterization of CdS nanowire synthesized by chemical bath deposition and wet chemical etching. *Appl. Surf. Sci.* 255, 6115–6120.
  32. Matsumura M., Furukawa S., Saho Y. & Tsubomura H. 1985 *J. Phys. Chem.*, 89, 1327.

33. Reber J. F. and Rusek M. 1986 *J. Phys. Chem.* 90, 824.
34. Jun Y.W., Choi J.S. & Cheon J. 2006 Shape control of semiconductor and metal oxide nanocrystals through nonhydrolytic colloidal routes. *Angew. Chem. Int. Ed* 45, 3414–3439.
35. Iqbal M., Ali A., Nahyoon N.R., Majeed A., Pothu R.K., Phulpoto S. & Thebo K. H. 2019 Photocatalytic degradation of organic pollutant with nanosized cadmium sulfide. *Materials Science for Energy Technologies* 2, 41–45
36. Miao J.J., Ren T., Dong L., Zhu J.J. & Chen H.Y. 2005 Double-template synthesis of CdS nanotubes with strong electrogenerated chemiluminescence. *Small* 1, 802–805.
37. Cao H.Q., Xu Y., Hong J., Liu H., Yin G., Li B., Tie C. & Xu Z. 2001 Sol-gel template synthesis of an array of single crystal CdS nanowires on a porous alumina template. *Adv. Mater.* 13, 1393–1394.
38. Jun Y.W., Lee S.M., Kang N.J. & Cheon J. 2001 Controlled synthesis of multi-armed CdS nanorod architectures using monosurfactant system. *J. Am. Chem. Soc.* 123, 5150–5151.
39. Tang K.-B., Qian Y.T., Zeng J.H. & Yang X.G., 2003 Solvothermal route to semiconductor nanowires. *Adv. Mater.* 15, 448.
40. Bunker C.E., Harruff B.A., Pathak P., Payzant A., Allard L.F. & Sun Y.P. 2004 Formation of cadmium sulfide nanoparticles in reverse micelles: extreme sensitivity to preparation procedure. *Langmuir* 20, 5642–5644.
41. Kar S. & Chaudhuri S. 2006 Selective growth of CdS one-dimensional nanostructures by a thermal evaporation process. *J. Phys. Chem. B* 110, 4542–4547.
42. Nakamoto, K. 1978 *Infrared and Raman Spectra of Inorganic and Coordination Compounds*, Wiley Online Library.
43. Khiew P. S., Huang N. M., Radiman S. & Ahmad M. S. 2004 synthesis and characterization of conducting polyaniline-coated cadmium sulphide nanocomposites in reverse microemulsion. *Materials Letters* 58, 516- 521.
44. Lu X., Gao H., Chen J., Chao D., Zhang W. & Wei Y. 2005 Poly (Acrylic Acid)- guided synthesis of helical polyaniline/CdS composite microwires. *Nanotechnology* 16, 113-117.
45. Das N.S., Ghosh P.K., Mitra M. K. & Chattopadhyay K.K. 2010 Effect of film thickness on the energy band gap of nanocrystalline CdS thin films analyzed by spectroscopic ellipsometry. *Phys. E Low-Dimens. Syst. Nanostruct.* 42, 2097–2102.
46. S. Kakarndee and S.Nanan, *J. Environ. Chem. Eng.* 6, 74(2005).
47. E. A. Rogozea, A.R. Petcu, N.L. Olteanu, C.A. Lazar, D. Cadar and M. Mihaly, *Mater. Sci. Semicond. Process.* 57, 1(2017).
48. M.A. Nazarkovsky, V.M. Bogatyrov, B. Czech, M.V. Galaburda, G. Wójcik, O.F. Kolomys, V.V. Strelchuk, M.L. Malysheva, O.I. Oranska and V.M. Gunko, *J. Photochem. Photobio. A: Chem.*, 334, 36(2017).
49. R.M. Mohamed. A.A. Ismail, M.W. Kadi, S. Ajayb, A.S. Alresheedi and I.A. Mkhallid, *ACS Omega*, 5, 33269(2020). <https://dx.doi.org/10.1021/acsomega.0c04969>
50. A. Kumar, M.K. Gora, G. Lal, B.L. Choudhary, P. L. Meena, R. S. Dhaka, R. R. Singhal, Sudhish Kumar and S. N. Dolia, *Environmental Science and Pollution Research*, 30, 18820(2023). <https://doi.org/10.1007/s11356-022-23420-y>.
51. S. Yi, X. Yue, D. Xu, Z. Liu, F. Zhao, D. Wang and Y. Lin, *New J. Chem.*, 39, 2917(2015). DOI: 10.1039/c4nj01738b
52. T. Senasu, K. Hemavibool and S. Nanan, *RSC Adv.*, 8, 22592(2018). DOI: 10.1039/c8ra02061b
53. D. Wang, C. Bao, Q. Luo, R. Yin, X. Li, J. An and Z. Xu, *J. Environ. Chem. Eng.*, 3, 1578(2015).
54. F. Sayilkan, S. Erdemoglu, M. Asilturk, M. Akarsu, S. Sener, H. Sayikan, M. Erdemoglu and E. Arpac, *Mater. Res. Bull.*, 41, 2276(2006).

#### Graphical Abstract

- CdS NPs prepared using facile solvothermal method.
- Prepared CdS NPs used for photodegradation of RB dye under visible light radiation.
- CdS NPs exhibited excellent photocatalytic activity and degraded 98.50% of RB dye in 80 min of light illumination.
- The prepared NPs demonstrated good stability and reusability, after fourth run of reuse 85% of activity retained.

